

Date of publication xxxx 00, 0000, date of current version June 12, 2022.

Digital Object Identifier 10.1109/TQE.2022.DOI

Stable Turnkey Laser System for a Yb/Ba Trapped Ion Quantum Computer

TIANYI CHEN¹, JUNKI KIM^{2,3}, MARK KUZYK², JACOB WHITLOW², SAMUEL PHIRI², BRAD BONDURANT², LEON RIESEBOS², KENNETH R. BROWN², and JUNGSANG KIM^{2,4},

¹Department of Physics, Duke University, Durham, NC 27708 USA

Corresponding author: Jungsang Kim (email: jungsang@duke.edu).

This work was supported by National Science Foundation STAQ project Phy-181891, National Science Foundation MRI award 1828154 and the U.S. Department of Energy Basic Energy Sciences award DE0019449. (*Tianyi Chen and Junki Kim are co-first authors.*)

ABSTRACT This work presents a stable and reliable turnkey continuous-wave laser system for a Yb/Ba multi-species trapped-ion quantum computer. The compact and rack-mountable optics system exhibits high robustness, operating over a year without realignment, regardless of temperature changes in the laboratory. The overall optical system is divided into a few isolated modules interconnected by optical fibers for easy maintenance. The light sources are frequency-stabilized by comparing their frequency with two complementary references, a commercial Fizeau wavelength meter and a high-finesse optical cavity. This scheme enables automatic frequency-stabilization for days with a sub-MHz precision.

INDEX TERMS Laser stability, optical design, quantum computing, trapped ions.

I. INTRODUCTION

RAPPED ions are a leading platform for quantum information science and technology as well as quantum computing [1]. This platform exhibits high fidelity quantum gates [2, 3, 4, 5, 6], wider connectivity between qubits[7, 8], and potential for realizing fault-tolerant quantum computation [9, 10, 11]. As the number of qubits and gates grow, the precise control of the system becomes more complex and it is critical to take a stable and engineered approach [12, 13]. In the context of quantum computing, the reliability of the components reduces the amount of required calibration and improves the duty cycle for data collection[7, 14, 15].

Manipulating and controlling trapped ion qubits relies on multiple laser beams interacting with the ions and thus reliable light sources are crucial parts of a trapped-ion-based quantum computer. A proper laser system should provide multiple colors of light, which are not only resilient to misalignment and mechanical vibrations but also well-stabilized to the atomic transition frequency of interest. Any spatial or spectral mismatch can lead to unsuccessful quantum computing operations, not only by errors in qubit state control, but also by inefficient ion loading and cooling, which increases the duty cycle of experiments.

Although the technique of building these optical system

functionalities with bulk optics has been known for a while, the increasing complexity of modern atomic experiments and the difficulty of maintaining long-term stability make it a challenging task. An optical system with a relatively large footprint assembled on an optical table is also sensitive to temperature changes, leading to misalignments among the components. To overcome the limited stability of typical optical systems, there have been several engineered approaches to build more stable systems for quantum technology [12, 13, 16, 17, 18]. Typical free-running external cavity diode lasers (ECDLs) feature linewidths ranging from kHz to MHz, while their central frequencies can drift over several MHz in a few seconds. The lasers can be locked to various frequency references, such as an atomic cell[19], a reference cavity[20, 21], other stabilized lasers[22, 23], and precise wavelength meter (WLM)[24, 25]. However, frequent manual intervention is often required since the traditional feedback mechanisms used to stabilize the laser frequency may not work over a broad frequency range. As trapped-ion quantum information experiments become larger and more complex, building a resilient and automated laser system with less human intervention is an essential but challenging task.

In this work, we designed and realized a stable turnkey laser system for a trapped-ion quantum computer. The sys-

²Department of Electrical and Computer Engineering, Duke University, Durham, NC 27708

³SKKU Advanced Institute of Nano Technology and Department of Nano Engineering, Sungkyunkwan University, Suwon, South Korea 16419

⁴IonQ, Inc., College Park, MD 20740



tem provides all required continuous-wave (CW) lights for manipulating and controlling both $^{171}\mathrm{Yb^{+}}$ and $^{138}\mathrm{Ba^{+}}$ ions. The compact design and active temperature stabilization significantly reduce the sensitivity to mechanical vibration and drifts in the environment. The lasers are frequency-stabilized and can be modulated easily. The spectral characterization shows that the lasers are locked within sub-MHz linewidth and their central frequencies are tunable over hundreds of MHz. The entire laser locking process is automated and can be controlled remotely through software.

II. SYSTEM DESIGN

Figure 1 represents a schematic of the laser system. While the reference cavity and the ion trap setup[26, 27, 28] are on an optical table, all the other parts, including ECDLs, other frequency references and optics, are mounted in standard 19-inch racks. The three circular arrows indicate the three stabilization feedback loops we implemented, each consisting of laser sources, laser distribution and modulation setup, frequency reference, electronics and laser controllers.

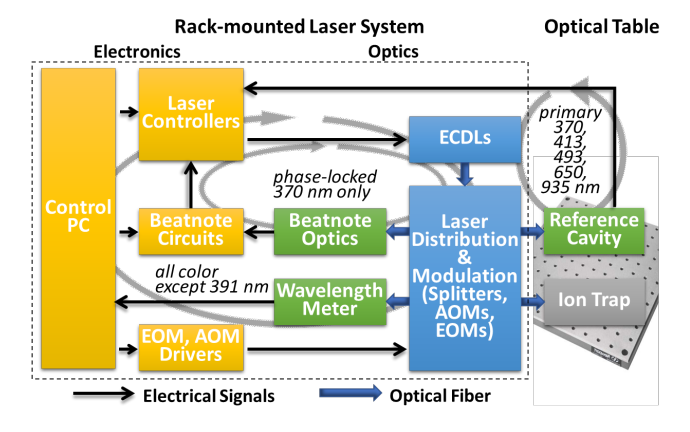


FIGURE 1. System Overview. Coherent light from the laser sources are modulated and distributed to the frequency references (green blocks) and the ion trap experimental apparatus (gray block) through optical fibers. The frequency references send feedback signals to laser controllers through electronics (yellow blocks). The three circular arrows indicate different stabilizing loops: cavity Pound-Drever-Hall (PDH) locking, beatnote phase-locking and wavelength meter (WLM)-assisted feedback. The label inside each arrow indicates which laser(s) is(are) stabilized by corresponding method. Switching between locking methods and changing feedback set-points are governed by a home-built software running on the personal computer (PC).

A. TARGET ION SPECIES AND LIGHT SOURCES

Our laser system supports an $^{171}{\rm Yb^+}/^{138}{\rm Ba^+}$ mixed-spices ion trap system. $^{171}{\rm Yb^+}$ has a nuclear spin of 1/2 that leads to hyperfine splitting in $^2{\rm S}_{1/2}$ ground state (Fig 2 (a)). The two magnetic-field insensitive sublevels (m $_F=0$) form a clock transition, adopted as long-lived qubit states[29, 30]. The simple hyperfine sublevel structure leads to efficient single-step qubit state preparation and less state leakage compared to other ion qubit candidates. In addition, the optical transitions utilized for ion trapping operations are easily achievable with direct diode lasers. The other species,

¹³⁸Ba⁺, can serve as coolant ions [11, 31, 32] in sympathetic cooling. Its nuclear spin is 0 and therefore there is no hyperfine structure. Its transition wavelengths lie within the visible wavelength range. They can also be easily accessed with diode lasers and are compatible with commercial fiberoptical components including modulators and splitters.

To manipulate and control those two ion species, 7 different wavelengths of light sources are needed. Figure 2 demonstrates the relevant energy levels. Yb neutral atoms can be ablated [33] from the Yb source and ionized to \$^{171}\$Yb^+\$ by a two-photon transition with 399 nm and 391 nm light, while Ba can be photo-ionized to \$^{138}\$Ba^+\$ by 413 nm light. Loaded \$^{171}\$Yb^+\$ (\$^{138}\$Ba^+\$) ions will then be Doppler cooled by 370 nm (493 nm) light with re-pumping light at 935 nm (650 nm). Doppler cooling, qubit state initialization and state discrimination [34, 35] of the \$^{171}\$Yb^+\$ qubit is done via 370 nm light, which is frequency modulated by electro-optic modulators (EOMs) and shuttered by acousto-optic modulators (AOMs). Quantum gates on \$^{171}\$Yb^+\$ qubits are performed by driving Raman transitions using a pulsed, frequency tripled Nd:YAG laser [36], which is not included in the laser system we depict.

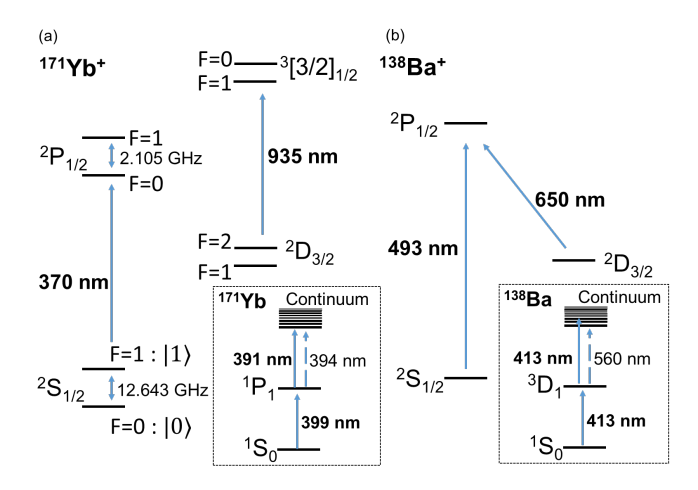


FIGURE 2. Level structures for target atomic ions, 171 Yb $^+$ (a) and 138 Ba $^+$ (b). The bold texts are the wavelengths supported by our laser system. The two magnetic-field insensitive states of 171 Yb $^+$ ions are adopted as the qubit states in the trapped-ion quantum computer.

6 external cavity diode lasers (ECDLs) and one laser diode (LD) provide all essential colors of light needed for this mixed-species ion trap system. Since the second photoionization 391 nm laser for ¹⁷¹Yb⁺ does not require narrow linewidth, a bare LD (Nichia, NDU4316) is used and directly coupled to an optical fiber. Other atomic transitions require a narrow laser linewidth, thus ECDLs with 100 kHz free-running linewidths are used. Four of the ECDLs (370 nm, 399 nm, 413 nm and 493 nm) are packaged in one rack-mounted module, along with isolators and fiber-coupling stages (Toptica, MDL pro). The other two ECDLs for 650 nm and 935 nm (AOSense, AOS-IF-ECDL), along with their isolators and fiber coupling stages, are packaged inside the beam distribution stage on the rack (Figure 3 (a)). Each ECDL has its own controller (Toptica, DLC pro and



AOSense, SILC-P-200) with a built-in proportional, integral and derivative (PID) servo to apply feedback on current and/or piezo voltage.

B. MECHANICALLY ROBUST OPTICAL SYSTEM

Most optical systems suffer from thermal drift which induces mechanical misalignment and thus intensity and frequency fluctuations. Recent works on engineering free-space optics[12, 16], prove that a proper apparatus design could lead to extended stability and reduce optical misalignment over time.

Our optical system is designed to operate for long periods of time without realignment. Each optical functional module is pre-designed using commercial computer-aided design (CAD) tools, minimizing mechanical degree of freedom to enhance stability. Each module is actively temperature-stabilized by a water cooling system to within $0.1^{\circ}C$. To examine the stability of our optics, we measure the beam pointing stability with a lateral-effect photo-diode sensor. The distance from the fiber launch to the detector is 450 mm and the change of the beam position is less than 1 um over 12 hours, which supports the robustness of our optical system. Recent data [37] also shows that such custom-designed optics could contribute to a longer laser coherence time in quantum computing comparing to previous report [7], in this case, from 83.3 ms to 494 ms.

The light beams generated from the sources are delivered to the laser distribution and modulation setup via optical fiber. The setup divides and distributes the light beams into several subsystems (Fig. 3 (a)(b)): the wavelength meter (WLM), the core ion trap chamber and frequency references for stabilization. The light beams are also modulated before being sent to the latter two subsystems, to drive specific atomic transitions or to provide essential sideband frequencies for the spectroscopy, respectively.

Most of the laser distribution and modulation system consist of fiber-based beam splitters and modulators, taking advantage of current fiber optics technology (Fig 3 (a)). Each light at 413 nm, 493 nm, 650 nm and 935 nm goes through two fiber splitters and one fiber EOM. Those fiber components are connected by butt coupling of fiber tips. The fiber EOMs have a broad modulation bandwidth (up to 6 GHz) and are actively temperature-stabilized by thermoelectric coolers to minimize thermal drift. Due to power broadening, 399 nm light does not need frequency modulation since it will not be stabilized to a reference cavity but only to the WLM. Its beam path is combined with 391 nm to ease optical alignment for Yb photoionization (Fig. 3 (a)).

On the other hand, near-UV 370 nm light, which drives the main transition of $^{171}{\rm Yb}^+$, is not compatible with fiber-based modulators and splitters due to its short wavelength and lack of supporting dielectric waveguide material. A separate custom-machined optics setup (Fig. 3 (b)(c)) is built for this specific wavelength. The optics are mounted on a water-cooled solid aluminum plate with predefined mounting holes. Low-profile optomechanics with low thermal expansion co-

efficient (Thorlabs Polaris series) are employed to reduce alignment instability caused by thermal drift. Once the optical alignment is completed, the assembly maintains a stable optical output power through single-mode fiber coupling for over a year without any realignment.

Unlike bulk optics, the CAD-based optical systems are easy to duplicate, enhancing the reproducibility of optics experiments. The design approach using CAD tools prevent potential mechanical conflicts without actually building it. Also, since all subsystems are modularized and connected by optical fibers, the impact of upgrading the optical layout or fixing misalignment will be confined to a module, which greatly reduces the maintenance workload.

C. FREQUENCY REFERENCES

External frequency references are essential to stabilize the laser frequencies near the atomic transition. The laser frequencies need to be maintained at the absolute atomic transition frequencies with linewidths well below the transition linewidths, typically tens of MHz for optical dipole transitions. To accomplish this, we adopted two complementary frequency references.

A Fabry-Perot type optical cavity (Stable Laser System, 6010-4) serves as a primary frequency reference via the Pound-Drever-Hall (PDH) locking technique[20, 21]. The optical cavity has multiple resonance frequencies with equal mode spacing and narrow linewidth, to which the lasers can be locked precisely. The cavity mirror coating covers the essential wavelengths with target finesse of 3000. It is installed in a vacuum chamber with a pressure of 10^{-8} Torr range to suppress refractive index fluctuation caused by air turbulence. The temperature of the vacuum chamber is actively stabilized near the zero-crossing temperature (35°C) of the ultra-low expansion glass (ULE) spacer of the cavity, where it features zero thermal expansion coefficient.

We built a custom mode-matching optical system to couple multiple outputs from ECDLs to the reference cavity (Fig. 4(a)). It is designed to couple 7 different wavelengths (¹⁷¹Yb⁺ transitions; 370 nm, 399 nm, 435 nm, 935 nm, ¹³⁸Ba⁺ transitions; 413 nm, 493 nm, 650 nm) to the single reference cavity. Each laser beam is frequency modulated by an EOM (see Fig. 3(a), Fig. 4(b)) before the fiber launch. Dichroic mirrors (DM) combine laser beams with different colors into the cavity mode and divide the reflected light into individual photodetectors (PDs).

To stabilize the laser frequency to an arbitrary set point, we used the offset-sideband locking method, adding a minor modification to the general Pound-Drever-Hall (PDH) technique[38]. On top of the PDH sideband (ω_{PDH}) for generating the error signal, an additional sideband modulation (ω_{offset}) is applied to the EOM to induce frequency offset (Fig. 4(c)). Those extra sidebands are locked to the cavity resonance. The broad bandwidth of fiber-based EOMs allow us to vary offset-sideband frequency over half of the cavity free-spectral range (FSR) of 1.5 GHz. Using this approach, we can stabilize the center frequency of the laser at the atomic

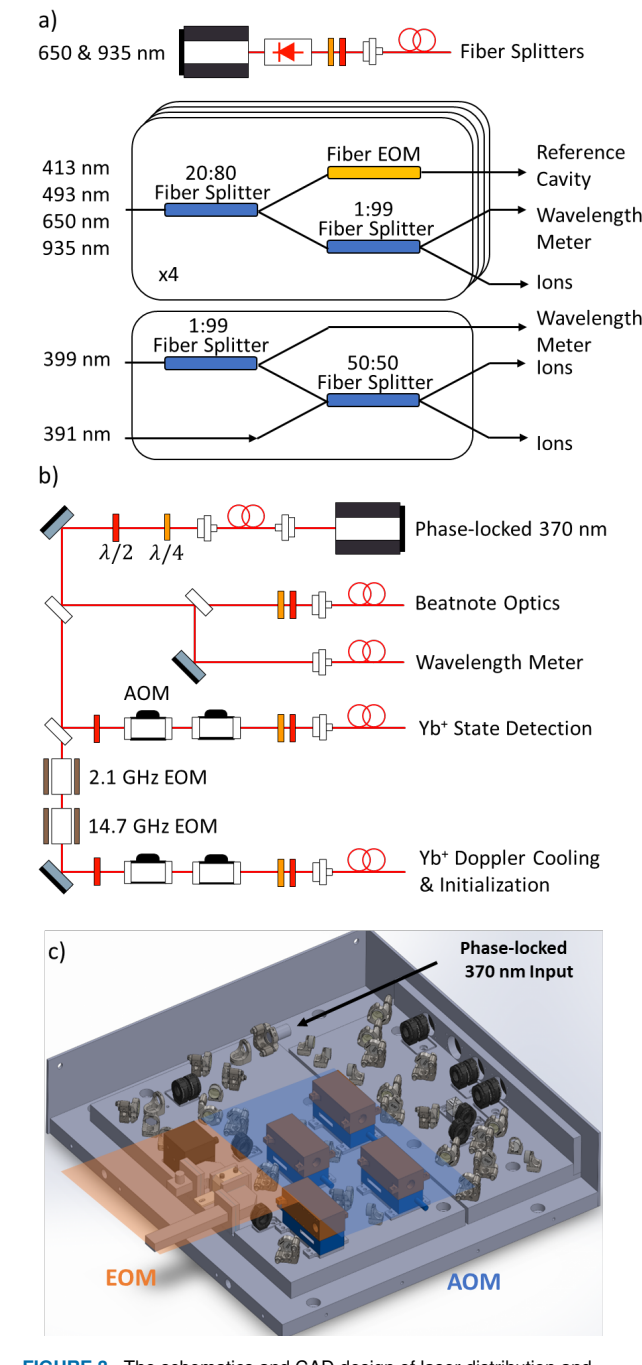


FIGURE 3. The schematics and CAD design of laser distribution and modulation. (a) ECDLs and fiber coupling stages for longer wavelengths (650 nm and 935 nm), as well as laser distribution for all lasers except 370 nm. (b) The simplified diagram of distribution and modulation for phase-locked 370 nm. Except the fibers connected to WLM, other fibers are PM fiber. (c) The separated distribution and modulation setup for 370 nm, using compact free-space optics. EOM: electro-optic modulator, AOM: acousto-optic modulator.

resonance, even if it is different from the cavity resonance. The PDH signal demodulation and feedback are carried out by the built-in field-programmable gate array (FPGA) based PID servo circuit in each laser's controller.

While this method works for most of the lasers, the mod-

ulation frequency for 370 nm light cannot be tuned over the FSR due to lack of fiber-based broadband EOMs at this wavelength. For 370 nm light, we adopted two ECDLs and set up a phase-locked loop between them instead [22, 23]. While the primary laser is PDH-locked to the cavity without an additional frequency offset, the phase-locked laser frequency is compared and locked at a programmable offset to the primary laser frequency by monitoring the beatnote between the two lasers. The frequency stabilization of the phase-locked laser is done by a simple phase-locked loop configuration (Fig. 4(d)). The frequency difference between the two lasers can be easily tuned by varying the reference RF frequency (ω_{ref}). We note that multiple phase-locked 370 nm lasers can be locked to a single primary laser. Their target frequencies can be tuned independently while the primary laser frequency remains unchanged.

Although the reference cavity provides excellent precision and stability, the feedback works only if the laser frequency is close enough to the target frequency. If the frequency difference is larger than PDH modulation frequency (25 MHz in our system), the demodulated error signal does not give negative feedback anymore and the laser cannot be locked. In the case of booting up the system or the laser being accidentally unlocked, operator intervention is typically needed to manually tune the laser frequency near the resonance in order to initiate the PDH lock. To automate this procedure, a precise wavelength meter (WLM) (HighFinesse, WS8-10) is adopted as the secondary frequency reference in our system.

Taking advantage of recent WLM technology, there have been a number of reports of using multi-channel WLMs as a frequency reference [24, 25]. In our setup, the WLM is regularly calibrated to a 780 nm reference ECDL laser to minimize the drift of WLM reading (every 4 hours). The reference laser is frequency stabilized to the rubidium 780 nm D2 line via Doppler-free saturated absorption spectroscopy (Toptica CoSy). The WLM has an 8-channel fiber switch and is able to read out the wavelength of each channel consecutively. The readout period over all eight channels is around 100 ms. The WLM has an absolute accuracy of about one MHz and has a working range covering hundreds of nm, enabling WLM-based laser frequency stabilization. However, its long acquisition time slows the feedback loop, especially when multiple lasers are locked at once through the fiber switch.

In this work, the WLM is used to decide which type of feedback is appropriate based on the difference between the WLM reading and the laser's target frequency (Fig. 5). This frequency error is constantly monitored via the WLM, regardless of the status of the lock. When the laser is in a wrong mode leading to very large errors (larger than a threshold value $\omega_{\rm TH,mode} = 2\pi \times 3$ GHz), the software will scan the laser piezo voltage until the correct mode is found. When the laser frequency is not close enough for the primary (PDH/beatnote) lock to work or the laser jumps out of the primary lock due to an external disturbance, the WLM-based feedback steps in to bring the laser frequency near the target.



The primary lock only kicks in when the error is smaller than the threshold ($\omega_{\rm TH}=2\pi\times 2$ MHz). A home-built Python program manages these procedures automatically and logs the WLM readings to the database.

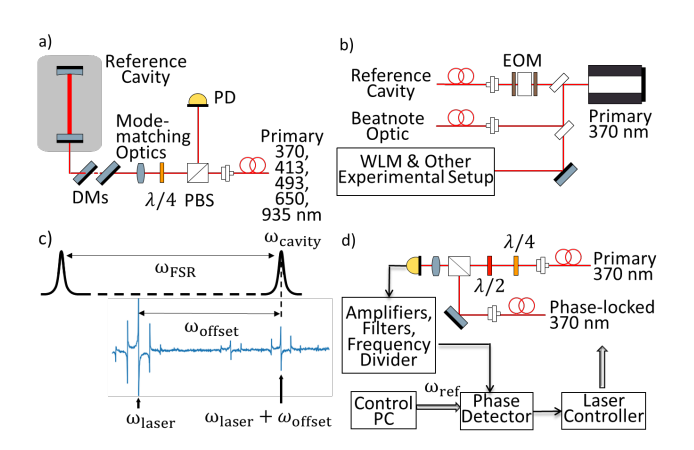


FIGURE 4. (a) The reference cavity installed in a vacuum chamber and corresponding optics setup for PDH signal generation. (b) The schematic for the distribution and modulation of primary 370 nm laser. (c) With the offset-sideband locking method, the laser sideband $\omega_{\text{laser}}+\omega_{\text{offset}}$ is locked to the cavity resonance ω_{cavity} . The laser frequency ω_{laser} can be stabilized. Its absolute frequency is also tunable by changing ω_{offset} . The cavity free spectral range is $\omega_{\text{FSR}}=2\pi\times1.5$ GHz. (d) The schematics for 370 nm beatnote phase-locking. PD: Photodiode, DMs: Dichroic mirrors, PBS: Polarizing beam splitter, FSR: Free-spectral range, PC: Personal computer.

III. CHARACTERIZATION OF LASER FREQUENCY STABILIZATION

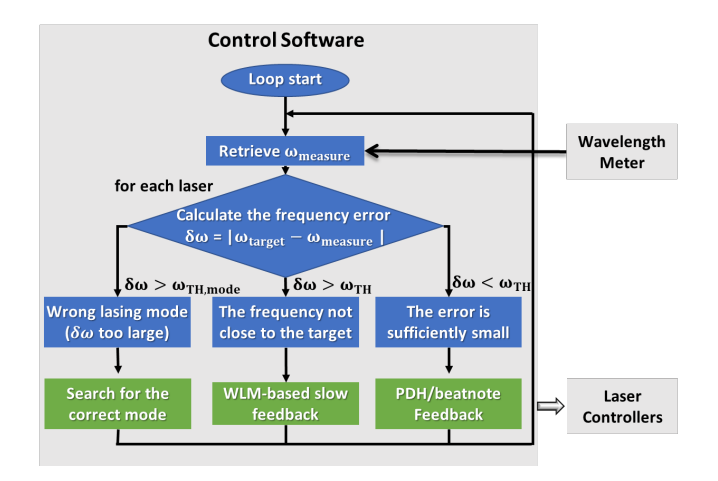


FIGURE 5. The control software monitors the WLM readings and decides the proper feedback method for each laser. The program retrieves ω_{measure} every 200 ms (80 ms) in switch mode (single mode). TH stands for threshold. A typical value we use for the threshold value is $\omega_{\mathrm{TH}}=2\pi\times 2$ MHz, $\omega_{\mathrm{TH,mode}}=2\pi\times 3$ GHz

Figure 6 presents multiple traces of PDH demodulated error signals. The measured linewidths of the cavity range from 385 kHz (935 nm) to 1.656 MHz (370 nm) and the derived finesses are from 3900 and to 906 respectively. Utilizing the built-in PID circuits of the laser controllers, we lock all five lasers to the same reference cavity. For the three shortwavelength lasers (370 nm, 413 nm, and 493 nm), the built-

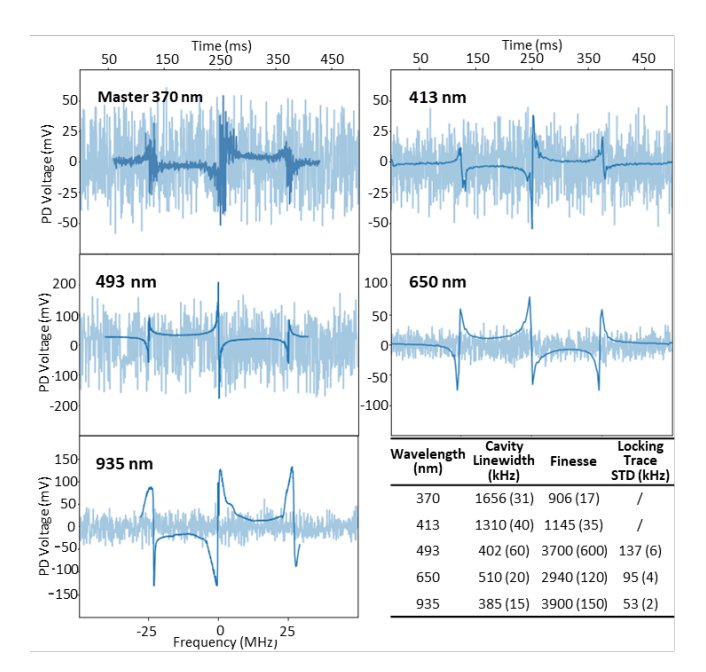


FIGURE 6. For each wavelength: PDH error signal while scanning the laser frequency around cavity resonance (dark blue), and the error signal in a time window when the PDH locking is enabled (light blue). (Table) Measured cavity linewidths, finesse and standard deviation (STD) of locking traces.

in PID bandwidth is limited to 30 kHz at most, leading to difficulty in reducing fast noise, while other controllers have a higher bandwidth of 1.5 MHz.

We investigated the Allan deviation[39] of the primary 370 nm laser to compare the performance of two frequency locking schemes (Fig. 7). One only relies on the WLM-based feedback and the other implements a PDH lock. During the PDH lock, the WLM only records the laser frequency without playing a role in the feedback loop. The Allan deviation is calculated from the time-stamped WLM readings, given by overlapped estimation;

$$\sigma^{2}(\tau) = \frac{1}{2(M-2n+1)} \sum_{j=0}^{M-2n} (\bar{y}_{j+n} - \bar{y}_{j})^{2}, \quad (1)$$

where $\{\bar{y}_i\}$ is normalized WLM readings in time-series, M is the total number of data points, and $\tau=n\Delta$ with the measurement time interval Δ . While the deviation in the WLM-based feedback lock is around 10^{-9} , the PDH lock demonstrates a more stable result, with at least one order of magnitude lower Allan deviation. The performance of PDH lock is already very close to Allan deviation measurement limit via WLM $(1.4\times10^{-10} \text{ with } 370 \text{ nm}, 3.6\times10^{-10} \text{ with } 935 \text{ nm})$, due to the resolution of the WLM (200 kHz). The increasing Allan deviation for PDH lock at long averaging times is due to WLM drifting, and not due to the instability of reference cavity or PDH lock.

While the lasers are tightly stabilized by the reference cavity, the WLM and home-built control software also provide a resilient laser system. Figure 8 presents the long-term trace of the WLM readings while the 493 nm laser

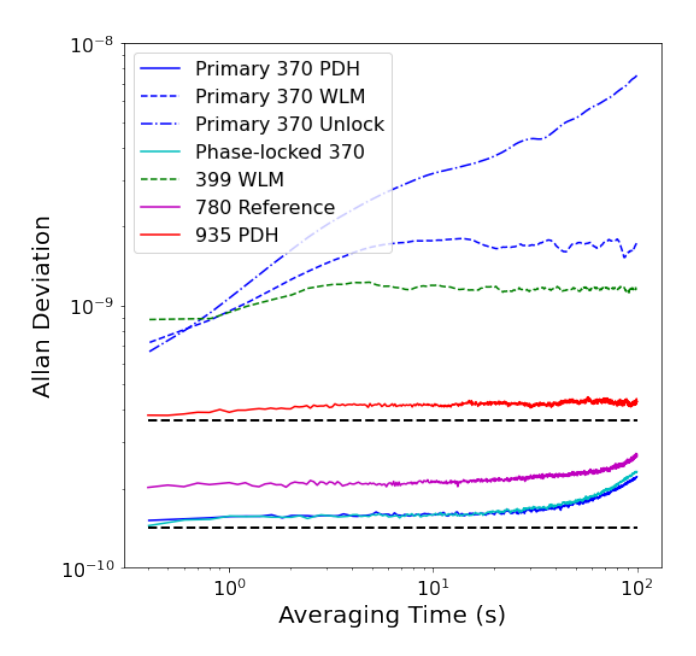


FIGURE 7. Allan deviation of 370,399,935,780 nm laser measured by WLM. The data points are collected every 400 ms. The slight increase of PDH lock trace is due to the WLM calibration drift. The readings of the 780 reference laser also show an increasing tail. The two black dashed horizontal lines (right below primary 370 PDH and 935 PDH) are the lowest achievable value calculated by simulating a noise uniformly distributed in the range of WLM resolution.

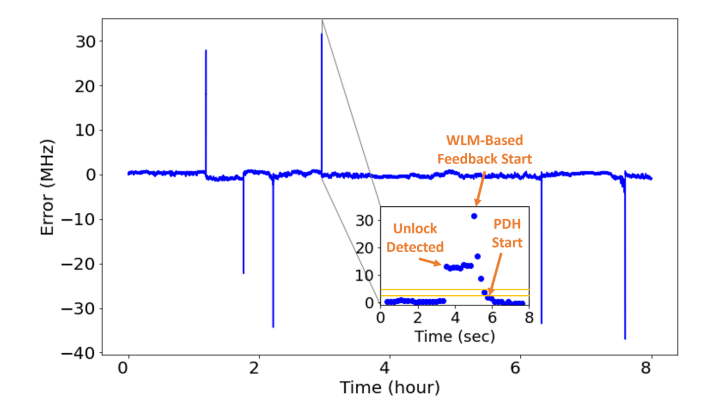


FIGURE 8. The locking trace of 493 nm laser monitored by WLM over 8 hours. The sharp spikes indicate the failure in PDH lock. When such an event is detected, the software will automatically switch to WLM-based feedback and restart PDH lock when it is ready. (subset) This recovery is typically done within a few seconds.

is locked. The laser is stabilized by the reference cavity most of the time. If the laser is accidentally unlocked from the PDH lock, the software will immediately recognize the event through the WLM reading and bring the laser back to near resonance. Once the laser is close enough, the PDH lock then kicks in to lock the laser with high stability. The procedure above is typically done in 3 seconds without any user intervention. Such self-sustaining frequency feedback control greatly eases the workload in daily experiments.

Our system also supports seamless tuning of the laser target frequency over hundreds of MHz, which would not be possible with only the cavity PDH lock. Whenever the target

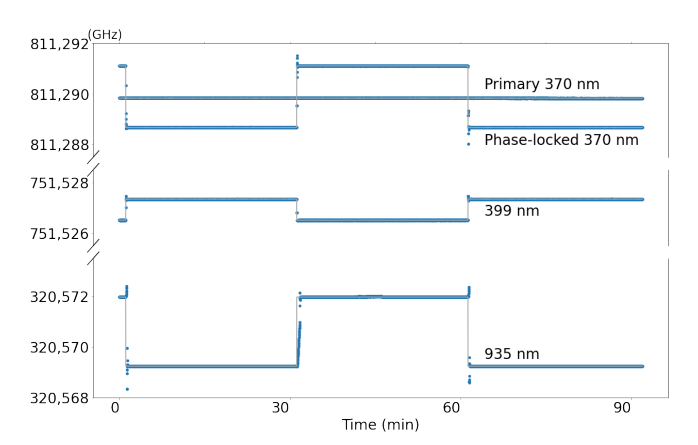


FIGURE 9. The logs of Yb⁺ lasers' frequencies while switching the target isotope between ¹⁷¹Yb⁺ and ¹⁷⁴Yb⁺ every 30 min. The lasers' set frequencies can be tuned over several GHz without manual re-adjustment. Such big adjustment can be done within 1 min.

frequency is set outside of the PDH lock range, the software will not only tune the laser to the new target frequency but also adjust the RF offset frequency for a new PDH/beatnote lock point. The synchronization between software and hardware is realized by an Advanced Real-Time Infrastructure for Quantum physics (ARTIQ) controller[40, 41]. Our homemade software runs in the ARTIQ Network Device Support Package (NDSP) framework. When the target frequency is updated via the ARTIQ interface, the software parameters and relevant hardware settings will update simultaneously. Fig. 9 shows the measured laser frequency as the target frequency is switched between the \$^{171}Yb^{+}\$ and \$^{174}Yb^{+}\$ resonances every 30 minutes. Although the target frequency differences for the two isotopes are around 3 GHz, locking to the new targets can be done within 1 minute. Note that the frequency difference exceeds the FSR of the cavity (1.5 GHz).

We performed spectroscopy of a single trapped ¹⁷⁴Yb⁺ ion as well (Fig.10). The ion is trapped and laser-cooled in a vacuum chamber. Then a short 370 nm laser detection pulse is applied. The scattered photons from the ion are collected by a high-NA (NA = 0.6) imaging lens and detected by single-photon detecting photomultiplier tubes (PMT). By varying the 370 nm laser frequency during the detection pulse, we measure the spectrum response of the single Yb ion. We present spectral measurements at different powers in Fig. 10. The ion temperature is measured to be 690 mK from fitting the peaks to a Doppler broadened Voigt profile. The high temperature is due to ion heating during the approximately 2 seconds time interval required to stabilize the laser when shifting from the Doppler-cooling frequency to the spectroscopy frequency. The 2 seconds interval is mainly occupied by WLM-based feedback since the frequency modulation is larger then $\omega_{\rm TH}$ (Fig. 5). Using a double-pass AOM could achieve a faster frequency modulation in this range, but we need a frequency shift of a few GHz to switch between ¹⁷¹Yb⁺ and ¹⁷⁴Yb⁺ (Fig. 9). In addition, during

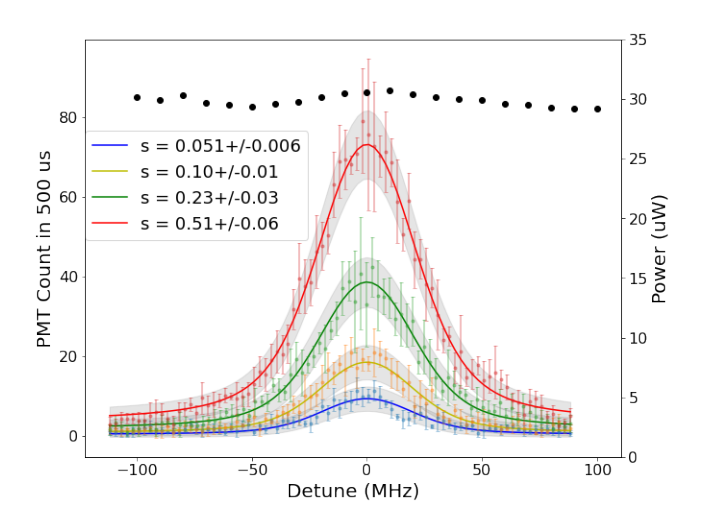


FIGURE 10. Ion fluorescence while scanning the 370 nm laser frequency. The laser frequency is scanned by changing the $\omega_{\rm ref}$ in beatnote locking subsystem. The black dots show the laser power during the scanning (right vertical axis). The the power fluctuation of 2-3% is observed even if the frequency remains fixed. The Voigt profile fits (solid lines) agree well with the expected natural linewidth of the atomic transition (19.6 MHz), power broadening as a function of the saturation parameter s, Doppler broadening (σ = 15.7 MHz, corresponding to 690 mK) and PMT collect efficiency (1.26%). Mean value is the average of 5 repeated measurements. The shaded area indicates the standard deviation of Poisson distribution for each trace.

the necessary ion-trap operations with ¹⁷¹Yb⁺ or ¹⁷⁴Yb⁺ (cooling, state initialization and discrimination), the 370 nm laser is fixed to one frequency and modulated by EOMs (Fig. 3 (b)). Thus, the long settling time for the frequency shift will not be an issue for quantum computing applications.

IV. DISCUSSION

In conclusion, we built a comprehensive and stable laser system for ion trapping experiments, which is robust and self-sustaining. The compact and actively temperature-stabilized optics system eliminated the need for optical realignment for over a year. Automated frequency stabilization using two complementary frequency references enables tight and resilient locking with extended tunability for each laser.

Optical fibers and fiber-based components provide great stability compared to free-space bulk optics, but the excess loss from fiber butt coupling is not negligible due to the small mode field diameter of the fiber, especially in the blue and UV. We measured the loss of FC/APC fiber connectors and found that it ranges from 3 dB to 7 dB per coupling depending on different combinations of fiber tip pairs. Also, slight mismatch in the axis of polarization-maintaining (PM) fibers induces polarization rotation which could lead to residual amplitude modulation noise in PDH locks, or after polarization cleanup at the output of the fiber[42, 43]. One could reduce this loss significantly by directly splicing fibers at the cost of sacrificing the system flexibility.

As for 370 nm light, we have not been able to find commercially available fiber-based, broadband electro-optic modulators. The transmission window of KTP crystal used for other short-wavelength light (413 nm) has a lower limit

of 350 nm. It is possible that proper engineering may enable all fiber-based control of 370 nm light in the future.

It has been observed that UV exposure for a long time period could degrade the quality of high-reflection (HR) coatings of the cavity mirrors[44, 45], which could harm the quality of the frequency stabilization. In our system, the cavity linewidth for UV wavelength has broadened to 8.3 MHz from 1.7 MHz after 1.5 years of operation. Such coating degradation is not unusual, but the mechanism and the solution are not well understood.

We believe our locking performance is mainly limited by the feedback controller bandwidth (16 kHz for 370, 413, 493 nm and 1.5 MHz for 650 and 935 nm). Nonetheless, the frequency stabilization is sufficient for the necessary ion-trap operations. A feedback circuit with a larger bandwidth may narrow the laser linewidth further to the order of a few tens of kHz.

While the software removes most of the need for human intervention, it sometimes fails to find the right mode within a certain amount of time because of the drift of the ECDL internal alignment. In this case, the software will send an error message and a human can adjust the laser current or temperature to recover the system remotely. This type of failure occurs once every 3 or 4 weeks. This failure could be minimized by temperature-stabilization of the laser heads.

In this work, we introduced our stable laser system, as well as potential approaches to upgrade the system. We expect this laser system could reduce the maintenance workload and enable scalability in trapped ion quantum computing systems.

V. ACKNOWLEDGEMENTS

This work was supported by National Science Foundation STAQ project Phy-181891, National Science Foundation MRI award 1828154 and the U.S. Department of Energy Basic Energy Sciences award DE0019449.

REFERENCES

- [1] Colin D Bruzewicz, John Chiaverini, Robert Mc-Connell, and Jeremy M Sage. Trapped-ion quantum computing: Progress and challenges. Applied Physics Reviews, 6(2):021314, 2019.
- [2] Emily Mount, Chingiz Kabytayev, Stephen Crain, Robin Harper, So-Young Baek, Geert Vrijsen, Steven T Flammia, Kenneth R Brown, Peter Maunz, and Jungsang Kim. Error compensation of single-qubit gates in a surface-electrode ion trap using composite pulses. Physical Review A, 92(6):060301, 2015.
- [3] John P Gaebler, Ting Rei Tan, Y Lin, Y Wan, Ryan Bowler, Adam C Keith, Scott Glancy, Kevin Coakley, Emanuel Knill, Dietrich Leibfried, et al. High-fidelity universal gate set for be 9+ ion qubits. Physical review letters, 117(6):060505, 2016.
- [4] CJ Ballance, TP Harty, NM Linke, MA Sepiol, and DM Lucas. High-fidelity quantum logic gates using



- trapped-ion hyperfine qubits. Physical review letters, 117(6):060504, 2016.
- [5] Raghavendra Srinivas, SC Burd, HM Knaack, RT Sutherland, Alex Kwiatkowski, Scott Glancy, Emanuel Knill, DJ Wineland, Dietrich Leibfried, Andrew C Wilson, et al. High-fidelity laser-free universal control of trapped ion qubits. Nature, 597(7875):209–213, 2021.
- [6] Craig R Clark, Holly N Tinkey, Brian C Sawyer, Adam M Meier, Karl A Burkhardt, Christopher M Seck, Christopher M Shappert, Nicholas D Guise, Curtis E Volin, Spencer D Fallek, et al. High-fidelity bell-state preparation with ca+ 40 optical qubits. Physical Review Letters, 127(13):130505, 2021.
- [7] Ye Wang, Stephen Crain, Chao Fang, Bichen Zhang, Shilin Huang, Qiyao Liang, Pak Hong Leung, Kenneth R Brown, and Jungsang Kim. High-fidelity twoqubit gates using a microelectromechanical-systembased beam steering system for individual qubit addressing. Physical Review Letters, 125(15):150505, 2020.
- [8] Kenneth Wright, Kristin M Beck, Sea Debnath, JM Amini, Y Nam, N Grzesiak, J-S Chen, NC Pisenti, M Chmielewski, C Collins, et al. Benchmarking an 11-qubit quantum computer. Nature communications, 10(1):1–6, 2019.
- [9] Laird Egan, Dripto M Debroy, Crystal Noel, Andrew Risinger, Daiwei Zhu, Debopriyo Biswas, Michael Newman, Muyuan Li, Kenneth R Brown, Marko Cetina, et al. Fault-tolerant control of an error-corrected qubit. Nature, 598(7880):281–286, 2021.
- [10] Ciaran Ryan-Anderson, JG Bohnet, Kenny Lee, Daniel Gresh, Aaron Hankin, JP Gaebler, David Francois, Alexander Chernoguzov, Dominic Lucchetti, NC Brown, et al. Realization of real-time faulttolerant quantum error correction. Physical Review X, 11(4):041058, 2021.
- [11] Lukas Postler, Sascha Heuβen, Ivan Pogorelov, Manuel Rispler, Thomas Feldker, Michael Meth, Christian D Marciniak, Roman Stricker, Martin Ringbauer, Rainer Blatt, et al. Demonstration of fault-tolerant universal quantum gate operations. Nature, 605(7911):675–680, 2022.
- [12] Ivan Pogorelov, Thomas Feldker, Ch D Marciniak, Lukas Postler, Georg Jacob, Oliver Krieglsteiner, Verena Podlesnic, Michael Meth, Vlad Negnevitsky, Martin Stadler, et al. Compact ion-trap quantum computing demonstrator. PRX Quantum, 2(2):020343, 2021.
- [13] SH Madkhaly, LA Coles, C Morley, CD Colquhoun, TM Fromhold, N Cooper, and L Hackermüller. Performance-optimized components for quantum technologies via additive manufacturing. PRX Quantum, 2(3):030326, 2021.
- [14] DPL Aude Craik, NM Linke, TP Harty, CJ Ballance, DM Lucas, AM Steane, and DTC Allcock. Microwave control electrodes for scalable, parallel, single-qubit

- operations in a surface-electrode ion trap. Applied Physics B, 114(1):3–10, 2014.
- [15] Holly N Tinkey, Craig R Clark, Brian C Sawyer, and Kenton R Brown. Transport-enabled entangling gate for trapped ions. Physical Review Letters, 128(5):050502, 2022.
- [16] Kai Frye, Sven Abend, Wolfgang Bartosch, Ahmad Bawamia, Dennis Becker, Holger Blume, Claus Braxmaier, Sheng-Wey Chiow, Maxim A Efremov, Wolfgang Ertmer, et al. The bose-einstein condensate and cold atom laboratory. EPJ Quantum Technology, 8(1):1, 2021.
- [17] Xiaowei Zhang, Jiaqi Zhong, Biao Tang, Xi Chen, Lei Zhu, Panwei Huang, Jin Wang, and Mingsheng Zhan. Compact portable laser system for mobile cold atom gravimeters. Applied Optics, 57(22):6545–6551, 2018.
- [18] Vladimir Schkolnik, Klaus Döringshoff, Franz Balthasar Gutsch, Markus Oswald, Thilo Schuldt, Claus Braxmaier, Matthias Lezius, Ronald Holzwarth, Christian Kürbis, Ahmad Bawamia, et al. Jokarus-design of a compact optical iodine frequency reference for a sounding rocket mission. EPJ Quantum Technology, 4(1):1–10, 2017.
- [19] Christopher J Foot. Atomic physics, volume 7. OUP Oxford, 2004.
- [20] RWP Drever, John L Hall, FV Kowalski, J_ Hough, GM Ford, AJ Munley, and H Ward. Laser phase and frequency stabilization using an optical resonator. Applied Physics B, 31(2):97–105, 1983.
- [21] DG Matei, T Legero, S Häfner, Ch Grebing, R Weyrich, W Zhang, L Sonderhouse, JM Robinson, J Ye, F Riehle, et al. 1.5 μ m lasers with sub-10 mhz linewidth. Physical review letters, 118(26):263202, 2017.
- [22] M. Prevedelli, T. Freegarde, and T. W. Hänsch. Phase locking of grating-tuned diode lasers. Applied Physics B, 60:S241, 1995.
- [23] U Schünemann, H Engler, R Grimm, M Weidemüller, and M Zielonkowski. Simple scheme for tunable frequency offset locking of two lasers. Review of Scientific Instruments, 70(1):242–243, 1999.
- [24] Luc Couturier, Ingo Nosske, Fachao Hu, Canzhu Tan, Chang Qiao, YH Jiang, Peng Chen, and Matthias Weidemüller. Laser frequency stabilization using a commercial wavelength meter. Review of Scientific Instruments, 89(4):043103, 2018.
- [25] Junwoo Kim, Keumhyun Kim, Dowon Lee, Yongha Shin, Sungsam Kang, Jung-Ryul Kim, Youngwoon Choi, Kyungwon An, and Moonjoo Lee. Locking multi-laser frequencies to a precision wavelength meter: Application to cold atoms. Sensors, 21(18):6255, 2021.
- [26] Peter Lukas Wilhelm Maunz. High optical access trap 2.0. Sandia National Laboratories, 1, 2016.
- [27] PB Antohi, D Schuster, GM Akselrod, J Labaziewicz, Y Ge, Z Lin, WS Bakr, and IL Chuang. Cryogenic ion trapping systems with surface-electrode traps. Review of Scientific Instruments, 80(1):013103, 2009.



- [28] Robert Fulton Spivey, Ismail Volkan Inlek, Zhubing Jia, Stephen Crain, Ke Sun, Junki Kim, Geert Vrijsen, Chao Fang, Colin Fitzgerald, Steffen Kross, et al. High-stability cryogenic system for quantum computing with compact packaged ion traps. IEEE Transactions on Quantum Engineering, 3:1–11, 2021.
- [29] C Langer, R Ozeri, John D Jost, J Chiaverini, B De-Marco, A Ben-Kish, RB Blakestad, Joseph Britton, DB Hume, Wayne M Itano, et al. Long-lived qubit memory using atomic ions. Physical review letters, 95(6):060502, 2005.
- [30] Ye Wang, Mark Um, Junhua Zhang, Shuoming An, Ming Lyu, Jing-Ning Zhang, L-M Duan, Dahyun Yum, and Kihwan Kim. Single-qubit quantum memory exceeding ten-minute coherence time. Nature Photonics, 11(10):646–650, 2017.
- [31] Murray D Barrett, B DeMarco, T Schaetz, V Meyer, D Leibfried, J Britton, J Chiaverini, WM Itano, B Jelenković, JD Jost, et al. Sympathetic cooling of 9 be+ and 24 mg+ for quantum logic. Physical Review A, 68(4):042302, 2003.
- [32] Ismail Volkan Inlek, Clayton Crocker, Martin Lichtman, Ksenia Sosnova, and Christopher Monroe. Multispecies trapped-ion node for quantum networking. Physical review letters, 118(25):250502, 2017.
- [33] Geert Vrijsen, Yuhi Aikyo, Robert F Spivey, I Volkan Inlek, and Jungsang Kim. Efficient isotope-selective pulsed laser ablation loading of 174 yb+ ions in a surface electrode trap. Optics Express, 27(23):33907– 33914, 2019.
- [34] Dietrich Leibfried, Rainer Blatt, Christopher Monroe, and David Wineland. Quantum dynamics of single trapped ions. Reviews of Modern Physics, 75(1):281, 2003.
- [35] Steve Olmschenk, Kelly C Younge, David L Moehring, Dzmitry N Matsukevich, Peter Maunz, and Christopher Monroe. Manipulation and detection of a trapped yb+ hyperfine qubit. Physical Review A, 76(5):052314, 2007.
- [36] WC Campbell, J Mizrahi, Q Quraishi, C Senko, D Hayes, D Hucul, DN Matsukevich, P Maunz, and C Monroe. Ultrafast gates for single atomic qubits. Physical review letters, 105(9):090502, 2010.
- [37] Chao Fang, Ye Wang, Shilin Huang, Kenneth R Brown, and Jungsang Kim. Crosstalk suppression in individually addressed two-qubit gates in a trapped-ion quantum computer. arXiv preprint arXiv:2206.02703, 2022.
- [38] James I Thorpe, K Numata, and J Livas. Laser frequency stabilization and control through offset sideband locking to optical cavities. Optics express, 16(20):15980–15990, 2008.
- [39] David W Allan. Statistics of atomic frequency standards. Proceedings of the IEEE, 54(2):221–230, 1966.
- [40] Sébastien Bourdeauducq, Robert Jördens, Peter Zotov, Joe Britton, Daniel Slichter, David Leibrandt, David Allcock, Aaron Hankin, Florent Kermarrec, Yann Sion-

- neau, Raghavendra Srinivas, Ting Rei Tan, and Justin Bohnet. Artiq 1.0, May 2016.
- [41] Grzegorz Kasprowicz, Paweł Kulik, Michal Gaska, Tomasz Przywozki, Krzysztof Pozniak, Jakub Jarosinski, Joseph W Britton, Thomas Harty, Chris Balance, Weida Zhang, et al. Artiq and sinara: Open software and hardware stacks for quantum physics. In Quantum 2.0, pages QTu8B–14. Optica Publishing Group, 2020.
- [42] W Zhang, MJ Martin, C Benko, JL Hall, J Ye, C Hagemann, T Legero, U Sterr, F Riehle, GD Cole, et al. Reduction of residual amplitude modulation to 1× 10-6 for frequency modulation and laser stabilization. Optics letters, 39(7):1980–1983, 2014.
- [43] Yinan Yu, Yicheng Wang, and Jon R Pratt. Active cancellation of residual amplitude modulation in a frequency-modulation based fabry-perot interferometer. Review of Scientific Instruments, 87(3):033101, 2016.
- [44] K Yamada, T Yamazaki, N Sei, R Suzuki, T Ohdaira, T Shimizu, M Kawai, M Yokoyama, T Mikado, T Noguchi, et al. Saturation of cavity-mirror degradation in the uv fel. Nuclear Instruments and Methods in Physics Research Section A: Accelerators, Spectrometers, Detectors and Associated Equipment, 393(1-3):44–49, 1997.
- [45] Christine E Geosling. Clean-cavity contamination in gas lasers. In 27th Annual Boulder Damage Symposium: Laser-Induced Damage in Optical Materials: 1995, volume 2714, pages 689–695. International Society for Optics and Photonics, 1996.

. . .